

Revealing Energy Dependence of Quantum Defects via Two Heteronuclear Atoms in an Optical Tweezer

Kunpeng Wang,^{1,2,3} Xiaodong He,^{1,2,*} Xiang Gao,^{4,5,†} Ruijun Guo,^{1,2,3} Peng Xu,^{1,2} Jun Zhuang,^{1,2,3} Runbing Li,^{1,2} Min Liu,^{1,2} Jin Wang,^{1,2} Jiaming Li,^{6,7,8} and Mingsheng Zhan^{1,2,‡}

¹*State Key Laboratory of Magnetic Resonance and Atomic and Molecular Physics, Wuhan Institute of Physics and Mathematics, Chinese Academy of Sciences - Wuhan National Laboratory for Optoelectronics, Wuhan 430071, China*

²*Center for Cold Atom Physics, Chinese Academy of Sciences, Wuhan 430071, China*

³*School of Physics, University of Chinese Academy of Sciences, Beijing 100049, China*

⁴*Institute for Theoretical Physics, Vienna University of Technology, A-1040 Vienna, Austria*

⁵*Beijing Computational Science Research Center, Beijing 100193, China*

⁶*Department of Physics and Center for Atomic and Molecular Nanosciences, Tsinghua University, Beijing 100084, China*

⁷*Key Laboratory for Laser Plasmas (Ministry of Education),*

and Department of Physics and Astronomy, Shanghai Jiao Tong University, Shanghai 200240, China

⁸*Collaborative Innovation Center of Quantum Matter, Beijing 100084, China*

(Dated: July 31, 2019)

As a physically motivated and computationally simple model for cold atomic and molecular collisions, the multichannel quantum defect theory (MQDT) with frame transformation (FT) formalism provides an analytical treatment of scattering resonances in an arbitrary partial wave between alkali-metal atoms, leading to the experimental observation of p - and d -wave resonances. However, the inconsistency of quantum defects for describing scattering resonances shows up when compared with experiments. Here, with two heteronuclear atoms in the ground state of an optical tweezer, the energy dependence of quantum defects is obviously revealed by comparing the measured s -wave scattering length with the prediction of MQDT-FT. By dividing the quantum defects into energy sensitive and insensitive categories, the inconsistency is ultimately removed while retaining the analytic structure of MQDT-FT. This study represents a significant improvement in the analytical MQDT-FT and demonstrates that a clean two-particle system is valuable to the test of collisional physics.

The tremendous progress in laser cooling, trapping and manipulating ultracold matters allows us to unveil a host of unique phenomena in quantum mechanical nature and thus attracts wide interest, reaching far into other fields, such as condensed matter and few- and many-body physics, beyond the atomic and molecular physics [1–4]. To determine the scattering properties and reveal the corresponding prospects of precise control of cold gaseous matter, a detailed understanding of the involved collision processes in the constituents is crucial. This can be obtained via a powerful yet analytical theoretical tool: the multichannel quantum defect theory (MQDT) [5–8]. This theory was initially developed by Seaton for atomic system with a long-range Coulomb interaction [4] and has been applied successfully for various atomic [6, 8, 9], and molecular collisions [7, 10–12], as well as cold atom and cold molecule collisions [13–15].

In particular, for the cold atom collisions, by replacing the numerical solutions for the long range potential with the analytic ones for the dominant Van der Waals interaction ($-C_6/R^6$) between pairs of neutral atoms [16], the scattering processes, including shape and Feshbach resonances, can be described by a set of three parameters: two eigenchannel quantum defects μ_α (singlet and triplet quantum defects μ_s and μ_t) that describe the scattering phase shifts at small inter-particle separations R and the dispersion coefficient C_6 that describes the potentials at

large R [17–21]. The predictive power of the analytic MQDT-FT, especially in search of resonances in p - and d -wave, has been proven experimentally [22–24]. However, the derived triplet quantum defects deviate from the ones offered by numerical coupled-channel calculations based on the full knowledge of the molecular potentials of the collisional pairs, e.g. for the case of ^{87}Rb - ^{85}Rb systems [22, 23, 25] and ^6Li - ^{133}Cs system [26].

To uncover more evidences of the underlying physics giving rise to the discrepancies between the MQDT-FT and experiments involved, complementary to the ones caught in studies of ^{87}Rb - ^{85}Rb magnetic Feshbach resonances, here we test the MQDT-FT by applying it to an inherently simplistic and seemingly straightforward problem, that is, determination of s -wave scattering lengths of open channels that has not yet been examined. Experimentally, such a scattering length is measured by utilizing an ultracold pair of ^{87}Rb - ^{85}Rb atoms with nearly perfect wavefunction overlap in a single optical tweezer, instead of the conventional bulk samples of cold atoms. To this end, we measure the microwave (MW) transition shifts for different scattering channels, and then deduce the associated scattering length from the analytical solution under the pseudopotential approximation. When comparing our measurements with predictions of MQDT-FT without adjusting quantum defects, discrepancies show up as encountered in experiments with Fesh-

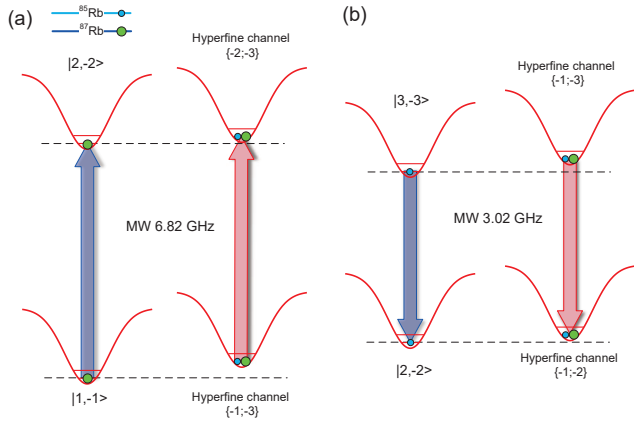


FIG. 1. Experimental scheme of the measurement of collisional shifts between ^{87}Rb and ^{85}Rb atoms in the motional ground states. (a) For the MW transition of ^{87}Rb , single atom transition starts from $|1, -1\rangle$ to $|2, -2\rangle$ and the involved channels in two atom collisions are $\{-1;-3\}$ and $\{-2;-3\}$. (b) For ^{85}Rb , single atom transition starts from $|3, -3\rangle$ to $|2, -2\rangle$ and the involved hyperfine channels in collisions are $\{-1;-3\}$ and $\{-1;-2\}$.

bach resonances. We find that the discrepancies originate from the energy dependence of quantum defects due to the contributions from $-C_8/R^8$ and $-C_{10}/R^{10}$ interactions outside the reaction zone, which are typically ignored in previous MQDT-FT. When we introduce two triplet quantum defects according to the energy sensitivity, the discrepancies can be resolved. Thus our explanation reveals the energy-dependence of quantum defects and can be extended to other complex dynamical processes and systems.

In the following, the scattering channels are defined by the internal states of ^{87}Rb ($q1$) and ^{85}Rb ($q2$), where the $q1$ ($q2$) denotes the quantum numbers of Zeeman sub-levels $|F, m_F\rangle$ of ^{87}Rb (^{85}Rb). A scattering channel is conveniently labeled by specifying the set of quantum numbers $\{q1; q2\}$ afterward (only include the m_F quantum number for brevity).

To experimentally deduce the scattering length, as shown in Fig. 1, we measure the resonant frequency difference of the MW transitions between two-atom collisions and the single-atom transitions. This scheme is free of the mean field shifts that are normally encountered in a bulk sample of cold atoms. When interrogating the ^{87}Rb atom, single-atom transition starts from $|F, m_F\rangle \equiv |1, -1\rangle$ to $|2, -2\rangle$, and the corresponding collisions start from $\{-1; -3\}$ channel to $\{-2; -3\}$. When interrogating ^{85}Rb , single-atom transition starts from $|3, -3\rangle$ to $|2, -2\rangle$, and the corresponding collisions start from $\{-1; -3\}$ channel to $\{-1; -2\}$. The main experimental details on the preparation of the ultracold sample of two atoms were described in ref. [27]. The corresponding resonant frequencies are measured by implementing the conven-

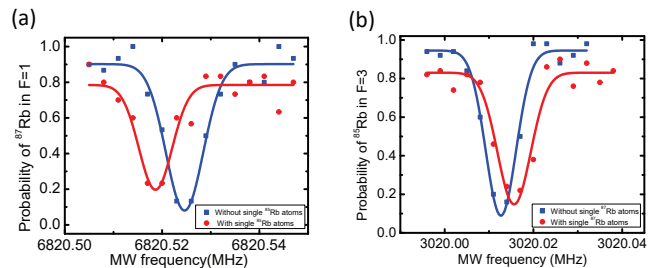


FIG. 2. Collisional shifts of single ^{87}Rb and ^{85}Rb atoms. (a) The measured MW resonant spectral of ^{87}Rb from $|1, -1\rangle$ to $|2, -2\rangle$ transition in the presence (red dots) and in the absence (blue squares) of ^{85}Rb in the $|3, -3\rangle$ state. (b) The measured MW resonant spectral of ^{85}Rb from $|3, -3\rangle$ to $|2, -2\rangle$ transition in the presence (red dots) and in the absence (blue squares) of ^{87}Rb in the $|1, -1\rangle$ state.

tional Rabi spectroscopy, which is an excellent probe for interacting cold atoms [28–30]. The spectroscopy on the ^{87}Rb (^{85}Rb) atom is implemented with a $120 \mu\text{s}$ (near π) MW pulse, as shown in Fig. 2(a) (Fig. 2(b)). For these measurements, the trap oscillation frequencies of single atoms are about 165 kHz and 27 kHz in the radial and axial directions respectively. As shown in Fig. 2(a), by comparing with that of a single ^{87}Rb , the resonant frequency is found to be reduced by 5.6 ± 1.0 kHz as colliding with a ^{85}Rb populated in the state of $|3, -3\rangle$, while the resonant frequency of ^{85}Rb atom is increased by 3.5 ± 1.3 kHz due to colliding with a ^{87}Rb atom in the state of $|1, -1\rangle$, as shown in Fig. 2(b). To efficiently extract the scattering lengths, we measure the frequency shifts of ^{87}Rb and ^{85}Rb atoms as functions of the trapping frequencies, as shown in the Fig. 3(a) and (b) respectively. We note that, the large measurement errors in transition frequencies are mainly caused by the fluctuations of magnetic field, since the Zeeman states involved are magnetic sensitive.

For the rubidium isotopes in a Gaussian optical tweezer with a wavelength of 852 nm, the difference in trap frequencies of the two atoms is only about 1% due to the slight difference in masses and the almost same trap depths (difference of 10^{-4}). The trapping frequencies of the two atoms are thus approximately equal so that the center of mass and relative motion are separable. We can thus straightforwardly adopt the analytical solutions for the dynamics of two trapped interacting ultracold atoms under the energy-independent delta pseudopotential approximation [31, 32] to evaluate the interaction energy. The pseudopotential approximation is valid provided that the van der Waals length scale $\beta_6 = (2\mu C_6/\hbar^2)^{1/4}$ is less than the radial harmonic-oscillator width $d_r = \sqrt{\hbar/(\mu\omega_r)}$, where μ is the reduced mass of the atom pair, ω_r is the angular trapping oscillation frequency in the radial direction, e.g. see refs. [33, 34]. For the measurements in Fig. 3(a) and (b),

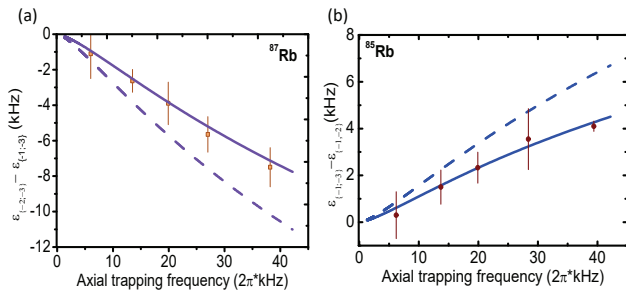


FIG. 3. The dependencies of collisional shifts experienced by ^{87}Rb atoms (see the left panel (a)) and ^{85}Rb atoms (b) on the axial oscillating frequencies. For (a) and (b), each dot is an average of 100-150 times of measurements. The accompanying error bars are statistic standard deviation for the average. The solid lines are fits to the Eq.(1) using the method of least-squares minimization and the dashed lines are the predictions of the shifts by adopting the values of quantum defects determined from precision spectroscopic measurements [25] as input parameters in the analytical MQDT-FT. See the main text for more details.

the smallest $d_r \approx 595 a_0$, and is much larger than the $\beta_6 \approx 165.1 a_0$, given the $C_6 \approx 4710$ a.u. (atomic units), where a_0 is the Bohr radius. Therefore all of the data adopted fulfill the aforementioned validity of pseudopotential approximation.

The ratio of the trapping frequencies in the radial and axial directions is $\eta \approx 6$. The derived relationship between collisional energy $\varepsilon_{\{q1;q2\}}$ and s -wave scattering length $a_{\{q1;q2\}}$ of scattering channel $\{q1;q2\}$ is given by

$$-\frac{\sqrt{\pi}}{a_{\{q1;q2\}}} = \mathcal{F}(-\varepsilon_{\{q1;q2\}}/2), \quad (1)$$

where $\mathcal{F}(-\varepsilon_{\{q1;q2\}}/2)$ denotes an implicit function of $\varepsilon_{\{q1;q2\}}$ [31, 32], and $\mathcal{F}(x) = -2\sqrt{\pi}\Gamma(x)/\Gamma(x-1/2) + \sqrt{\pi}\Gamma(x)/\Gamma(x+1/2) \sum_{m=1}^{n-1} F(1, x; x+1/2; \exp(i2\pi m/n))$, where $F(a,b;c;x)$ denotes the hypergeometric function, and n is a positive integer, here $n = \eta \approx 6$. Thus, Eq.(1) relates the $a_{\{q1;q2\}}$ to the collisional energy $\varepsilon_{\{q1;q2\}}$.

Given one of the scattering length of the associated channels, e.g. $\{-2;-3\}$ channel [35], the actual collisional energy $\varepsilon_{\{-2;-3\}}$ can be calculated by using the Eq.(1), and thus the $\varepsilon_{\{-1;-3\}}$ of the channel to be measured can be deduced from the measured frequency shifts. Ultimately, the scattering length $a_{\{-1;-3\}}$ can be extracted by fitting the data points in Fig. 3(a) to the Eq.(1).

The associated scattering channels in the Fig. 3(a) are $\{-2;-3\}$ and $\{-1;-3\}$, therefore the measured frequencies amounts to the difference between two interaction energies $\varepsilon_{\{-2;-3\}}$ and $\varepsilon_{\{-1;-3\}}$. Given the measured value of $a_{\{-2;-3\}} = 213(7) a_0$ in the previous work [35], the data in Fig. 3(a) are fitted to Eq. (1) via least-squares minimization yielding $a_{\{-1;-3\}} = 3.2(5) \times 10^2 a_0$, as shown by the solid line. Then we turn to the collisional shifts of

^{85}Rb atoms, as shown in Fig. 3(b), which associate with the differences between two other interaction energies, and for scattering channels $\varepsilon_{\{-1;-2\}}$ and $\varepsilon_{\{-1;-3\}}$, respectively. Given the calculated $a_{\{-1;-2\}} = 229.4 a_0$ via a coupled channel method [25], the other measured value of $a_{\{-1;-3\}}$ is similarly extracted from the same fitting function as $3.0(5) \times 10^2 a_0$, as the solid line shown in Fig. 3(b). The average value of $a_{\{-1;-3\}} = 3.1(5) \times 10^2 a_0$. This measurement matches the coupled channel calculations using the MOLSCAT package [36] with the precise interaction potentials derived from high precision molecular spectroscopy [25].

Subsequently following the analytical MQDT-FT approach [17] and adopting the $\{\mu_s, \mu_t\} \approx \{0.7253, 0.1822\}$ determined from precision spectroscopic measurements [25], we found that the calculated scattering length $a_{\{-1;-3\}}$ is obviously overestimated, as shown in Table I. To intuitively illustrate such a discrepancy, the calculated corresponding dependence of collisional shifts seen by ^{87}Rb on the axial trapping frequencies is plotted as the dashed lines shown in Fig. 3(a), as well as the similar behavior encountered in ^{85}Rb shown in Fig. 3(b). Additionally, we also calculate the scattering length of channel $\{-1;-2\}$, given the same input parameters of μ_s and μ_t , similar discrepancies show up, as shown in Table I. Interestingly, using the μ_t determined by another cold atom experiments [22], the calculated scattering lengths for these two elastic channels are both underestimated, as shown in Table I.

In the analytical framework of the MQDT-FT with only C_6 type of long-range potential, one need to choose a very large reaction zone where the C_8, C_{10} interactions are negligible. But after carrying out a careful check for the Rb_2 interaction potentials [25], we find out that the long-range C_8 and C_{10} potentials play a crucial role in determining the values of scattering lengths in the region $20 a_0 \leq R \leq 45 a_0$, where the effective momentum for channels with high dissociative thresholds may be comparable with the contributions of C_8 and C_{10} interactions, leading that the μ_α of these eigenchannels [37] are much more sensitive to the channel energy than other eigenchannels. Based on the phase amplitude method or the Wentzel-Kramers-Brillouin (WKB) approximation, the eigen quantum defect μ_α closely related with the inverse (approximately) of the local effective momentum of each channel within the reaction zone [13]. Then one would expect a strong perturbation to μ_α if there exists closed channels with the zero of their local effective momentum $k(R)$ within the extended reaction zone. Therefore, after the extension of the reaction zone, the original eigen quantum defect μ_α will change by $\delta\mu_\alpha$, which represents the corrections due to the high-order long-range potentials, and may strongly depend on the channel energies.

Based on the conventional MQDT, the scattering state wavefunctions can be expressed as superpositions of eigenchannel wavefunctions Ψ_α characterizing the de-

TABLE I. List of scattering lengths for $\{-1;-3\}$ and $\{-1;-2\}$ channels. The resulting scattering lengths are divided into two groups by adopting two different sets of input parameters of $\{\mu_s, \mu_t\}$ for the MQDT-FT, from up to down, the values of $\{\mu_s, \mu_t\}$ are respectively adopted from ref. [25] and ref. [22]. And each group is compared to both the measured result and coupled-channel calculations. See the main text for more details. The scattering lengths are in units of a_0 .

Channel	μ_s	μ_t	$a_{MQDT-FT}$	a_{exp}	a_{CC}
$\{-1;-3\}$	0.7253	0.1822	420.2	$3.1(5)\times 10^2$	314.8
$\{-1;-2\}$	0.7253	0.1822	242.5		229.4
$\{-1;-3\}$	0.7253	0.2045	277.4	$3.1(5)\times 10^2$	314.8
$\{-1;-2\}$	0.7253	0.2045	207.7		229.4

TABLE II. List of improved scattering lengths for $\{-1;-3\}$ and $\{-1;-2\}$ channels. The resulting scattering lengths are calculated by adopting the improved set of parameters $\{\mu_s^{EI}, \mu_t^{EI}, \mu_t^{ES}\}$ and are compared with both the measured result and coupled-channel calculations. See the main text and Supplemental Material for more details.

Channel	μ_s^{EI}	μ_t^{EI}	μ_t^{ES}	$a_{MQDT-FT}$	a_{exp}	a_{CC}
$\{-1;-3\}$	0.7253	0.1822	0.1984	315.0	$3.1(5)\times 10^2$	314.8
$\{-1;-2\}$	0.7253	0.1822	0.1984	234.3		229.4

tailed dynamics within the reaction zone with a common short-range phase shift, which relates to the eigenchannel quantum defect μ_α by $\pi\mu_\alpha$. It was customarily expected that the μ_α is almost independent of the channel energies, e.g. see Refs. [17, 22, 23]. However, from the above arguments, to retain the analytic structure of MQDT-FT and meanwhile remove the differences between theoretical and experimental results on the scattering lengths, we propose to divide the eigenchannels into two categories: the energy insensitive (EI) one and the energy sensitive (ES) one.

For our interested $\{-1;-3\}$ elastic scattering process, the singlet (0, 0; 4, -4) and triplet (1, 0; 4, -4) eigenchannels are almost correlated with the two fragmentation channels with the two lowest dissociative thresholds, the zero point of their $k(R)$ are larger than $45 a_0$ and the C_8 and C_{10} potentials will generally influence their $k(R)$ within the reaction zone by less than 10%. We classify them into the EI category, the corresponding values of μ_s^{EI} and μ_t^{EI} remain 0.7253 and 0.1822, respectively. On the other hand, the remaining two triplet (1,-1; 3,-3) and (1,-1; 4,-3) eigenchannels are correlated with the two highest dissociative thresholds, the zero point of their $k(R)$ are at about $41 a_0$ and the influence of C_8 and C_{10} potential can be larger than 50%. We then classify them into the ES category, where a slightly different value $\mu_t^{ES} \approx 0.1984$ is assigned. Similarly, we use the same classification standard and the related μ_α values for the $\{-1;-2\}$ scattering process with total $M=-3$. As shown in Table II, the resulting scattering lengths for both $\{-1;-3\}$ and $\{-1;-2\}$ channels are significantly improved and in good agreement with our experimental measurement and the coupled-channel calculations.

To confirm the plausibility of our proposal to introduce the energy dependence of quantum defects, we also carried out some numerical studies for calculating the eigenchannel quantum defects from first-principle, in a

similar spirit of what we did in atomic system [38]. The preliminary results have confirmed the correctness of our classification of μ_t into the energy sensitive and insensitive ones, hence this study represents a significant improvement in the analytical MQDT-FT.

Extending the improved MQDT-FT scenario to the analysis of Feshbach resonances in ultracold ensembles is straightforward [22–24, 26]. In general, the scattering length measurement technique introduced here can be used to test the theoretical models of collisions beyond the neutral atoms [28–30], such as atom-molecule and molecule-molecule scattering processes. Furthermore, the present work sets the stage for experiments with a deterministically prepared two-particle system in which clean collisional dynamics and Feshbach resonances can be further explored.

We acknowledge E. Tiemann for his coupled-channel calculation results on the scattering lengths. We also thank L. You for fruitful discussions. This work was supported by the National Key Research and Development Program of China under Grant No. 2017YFA0304501, No. 2016YFA0302104, No. 2016YFA0302800, and No. 2016YFA0302002, the National Natural Science Foundation of China under Grant No. 11774389, No. 11774023 and No. U1530401, the Strategic Priority Research Program of the Chinese Academy of Sciences under Grant No. XDB21010100 and the Youth Innovation Promotion Association CAS No. 2019325.

* hexd@wipm.ac.cn

† xiang.gao@tuwien.ac.at

‡ mszhan@wipm.ac.cn

[1] I. Bloch, J. Dalibard, and W. Zwerger, Many-body physics with ultracold gases, Rev. Mod. Phys. **80**, 885 (2008).

- [2] C. Chin, R. Grimm, P. Julienne, and E. Tiesinga, Feshbach resonances in ultracold gases, *Rev. Mod. Phys.* **82**, 1225 (2010).
- [3] M. A. Baranov, M. Dalmonte, G. Pupillo, and P. Zoller, Condensed Matter Theory of Dipolar Quantum Gases, *Chem. Rev.* **112**, 5012 (2012).
- [4] C. Greene, P. Giannakeas, and J. Pérez-Ríos, Universal few-body physics and cluster formation, *Rev. Mod. Phys.* **89**, 035006 (2017).
- [5] M. J. Seaton, Quantum defect theory, *Rep. Prog. Phys.* **46**, 167 (1983).
- [6] U. Fano, Unified treatment of perturbed series, continuous spectra and collisions, *J. Opt. Soc. Am.* **65**, 979 (1975).
- [7] C. H. Greene, and Ch. Jungen, Molecular Applications of Quantum Defect Theory, *Adv. At. Mol. Phys.* **21**, 51 (1985).
- [8] M. Aymar, C. H. Greene, and E. Luc-Koenig, Multichannel Rydberg spectroscopy of complex atoms, *Rev. Mod. Phys.* **68**, 1015 (1996).
- [9] C. M. Lee, and K. T. Lu, Spectroscopy and Collision Theory. II. The Ar Absorption Spectrum, *Phys. Rev. A* **8**, 1241 (1973).
- [10] Ch. Jungen, and G. Raseev, Spin-electronic-rotational frame transformation for photoionization and Rydberg spectra of diatomic molecules, *Phys. Rev. A* **57**, 2407 (1998).
- [11] X. Gao, W. H. Zhang, Y. X. Mo, and J. M. Li, Application of multichannel quantum defect theory to unveil quantum interferences in dissociation of superexcited F_2 , *Phys. Rev. A* **82**, 031401(R) (2010).
- [12] U. Fano, Quantum defect theory of l uncoupling in H_2 as an example of channel-interaction treatment, *Phys. Rev. A* **2**, 353 (1970).
- [13] J. P. Burke, C. H. Greene, and J. L. Bohn, Multichannel Cold Collisions: Simple Dependences on Energy and Magnetic Field, *Phys. Rev. Lett.* **81**, 3355 (1998).
- [14] Z. Idziaszek, and P. S. Julienne, Universal Rate Constants for Reactive Collisions of Ultracold Molecules, *Phys. Rev. Lett.* **104**, 113202 (2010).
- [15] J. F. E. Croft, J. M. Hutson, and P. S. Julienne, Optimized multichannel quantum defect theory for cold molecular collisions, *Phys. Rev. A* **86**, 022711 (2012).
- [16] B. Gao, Solutions of the Schrödinger equation for an attractive $1/r^6$ potential, *Phys. Rev. A* **58**, 1728 (1998).
- [17] B. Gao, E. Tiesinga, C. J. Williams, and P. S. Julienne, Multichannel quantum-defect theory for slow atomic collisions, *Phys. Rev. A* **72**, 042719 (2005).
- [18] T. M. Hanna, E. Tiesinga, and P. S. Julienne, Prediction of Feshbach resonances from three input parameters, *Phys. Rev. A* **79**, 40701 (2009).
- [19] B. Gao, Analytic description of atomic interaction at ultracold temperatures: The case of a single channel, *Phys. Rev. A* **80**, 012702 (2009).
- [20] B. Gao, Analytic description of atomic interaction at ultracold temperatures. II. Scattering around a magnetic Feshbach resonance, *Phys. Rev. A* **84**, 022706 (2011).
- [21] B. P. Ruzic, C. H. Greene, and J. L. Bohn, Quantum defect theory for high-partial-wave cold collisions, *Phys. Rev. A* **87**, 32706 (2013).
- [22] S. Dong, Y. Cui, C. Shen, Y. Wu, M. K. Tey, L. You, and B. Gao, Observation of broad p -wave Feshbach resonances in ultracold ^{85}Rb - ^{87}Rb mixtures, *Phys. Rev. A* **94**, 062702 (2016).
- [23] Y. Cui, C. Shen, M. Deng, S. Dong, C. Chen, R. L. B. Gao, M. K. Tey, and L. You, Observation of Broad d -Wave Feshbach Resonances with a Triplet Structure, *Phys. Rev. Lett.* **119**, 203402 (2017).
- [24] X.-C. Yao, R. Qi, X.-P. Liu, X.-Q. Wang, Y.-X. Wang, Y.-P. Wu, H.-Z. Chen, P. Zhang, H. Zhai, Y.-A. Chen, and J.-W. Pan, Degenerate Bose gases near a d -wave shape resonance, *Nat. Phys.* **15**, 570 (2019).
- [25] C. Strauss, T. Takekoshi, F. Lang, K. Winkler, R. Grimm, J. Hecker Denschlag, and E. Tiemann, Hyperfine, rotational, and vibrational structure of the $a^3\Sigma_u^+$ state of $^{87}\text{Rb}_2$, *Phys. Rev. A* **82**, 052514 (2010).
- [26] R. Pires, M. Repp, J. Ulmanis, E. D. Kuhnle, M. Weidemüller, T. G. Tiecke, C. H. Greene, B. P. Ruzic, J. L. Bohn, and E. Tiemann, Analyzing Feshbach resonances: A ^6Li - ^{133}Cs case study, *Phys. Rev. A* **90**, 012710 (2014).
- [27] K. Wang, X. He, R. Guo, P. Xu, C. Sheng, J. Zhuang, Z. Xiong, M. Liu, J. Wang, and M. Zhan, Preparation of a Hetero-nuclear Two-atom System in the 3D Motional Ground State in an Optical Tweezer, Preprint at <https://arxiv.org/abs/1902.04284> (2019).
- [28] G. K. Campbell, J. Mun, M. Boyd, P. Medley, A. E. Leanhardt, L. G. Marcassa, D. E. Pritchard, and W. Ketterle, Imaging the Mott Insulator Shells by Using Atomic Clock Shifts, *Science* **313**, 649 (2006).
- [29] L. Franchi, L. F. Livi, G. Cappellini, G. Binella, M. Inguscio, J. Catani, and L. Fallani, State-dependent interactions in ultracold ^{174}Yb probed by optical clock spectroscopy, *New J. Phys.* **19**, 103037 (2017).
- [30] A. Goban, R. B. Hutson, G. E. Marti, S. L. Campbell, M. A. Perlin, P. S. Julienne, J. P. DIncao, A. M. Rey, and J. Ye, Emergence of multi-body interactions in a fermionic lattice clock, *Nature* **563**, 369 (2018).
- [31] Z. Idziaszek, and T. Calarco, Two atoms in an anisotropic harmonic trap, *Phys. Rev. A* **71**, 050701(R) (2005).
- [32] Z. Idziaszek, and T. Calarco, Analytical solutions for the dynamics of two trapped interacting ultracold atoms, *Phys. Rev. A* **74**, 022712 (2006).
- [33] D. Blume, and C. H. Greene, Fermi pseudopotential approximation: Two particles under external confinement, *Phys. Rev. A* **65**, 043613 (2002).
- [34] E. L. Bolda, E. Tiesinga, and P. S. Julienne, Effective-scattering-length model of ultracold atomic collisions and Feshbach resonances in tight harmonic traps, *Phys. Rev. A* **66**, 013403 (2002).
- [35] I. Bloch, M. Greiner, O. Mandel, T. W. Hansch, and T. Esslinger, Sympathetic cooling of ^{85}Rb and ^{87}Rb , *Phys. Rev. A* **64**, 021402(R) (2001).
- [36] J. M. Hutson, and C. R. Le Sueur, MOLSCAT: A program for non-reactive quantum scattering calculations on atomic and molecular collisions. *Comput. Phys. Commun.* **241**, 9 (2019).
- [37] see the Supplemental Material for more details.
- [38] X. Gao, X. Y. Han, and J. M. Li, Intimate relationship between spectroscopy and collisions: a scenario to calculate relevant atomic data for astrophysics. *J. Phys. B: At. Mol. Opt. Phys.* **49**, 214005 (2016).

Supplemental Material

Details of Multichannel Quantum Defect Theory Calculation

For two colliding alkali-metal atoms in their ground states, the eigenchannels can be simply denoted as $(S, M_s; I, M_I)$, where $S=s_1+s_2$ and $I=i_1+i_2$ are the total electronic spin and nuclear spin of the two atoms respectively, and M_s and M_I are the corresponding projection of them on the interatomic axis respectively. Since $s_1=s_2=1/2$, we have singlet and triplet eigenchannels, the corresponding quantum defects are described by μ_s and μ_t , respectively, denoted as $\mu_\alpha = \{\mu_s, \mu_t\}$. When the colliding atoms outside the reaction zone, the eigenchannel wavefunctions Ψ_α as can also be expressed as superpositions of fragmentation channels wavefunctions Φ_i . For present elastic scattering channel of $\{-1; -3\}$ with total $M = -4$, there are four eigenchannels involved, namely, $(0, 0; 4, -4)$, $(1, 0; 4, -4)$, $(1, -1; 3, -3)$ and $(1, -1; 4, -3)$, which relate to the fragmentation channel $\{-1; -3\}$ by the superposition coefficients $U_{i\alpha}$, reflecting the detailed interaction dynamics. Under the FT approximation [1–3], $U_{i\alpha}$ can be simply calculated by the geometric recoupling coefficients, i.e.

$$U_{i\alpha} = \langle F_1^i M_{F_1}^i F_2^i M_{F_2}^i | S^\alpha M_S^\alpha I^\alpha M_I^\alpha \rangle \quad (1)$$

It should be mentioned that although the FT are broadly used in atomic [2, 4], molecular [1, 5, 6] and cold atom collision problems [3, 7, 8] with great success, there exists some differences with the ab-initio calculation results [2, 9].

From the eigenchannel parameters of μ_α and $U_{i\alpha}$, the short-range scattering matrix K_{ij}^c is expressed as [10]:

$$K_{ij}^c = \sum_\alpha U_{i\alpha} \tan(\pi\mu_\alpha + \pi/8) U_{j\alpha}. \quad (2)$$

For our interested scattering channel $\{-1; -3\}$, the effective one open channel short-range scattering matrix K_{eff}^c is obtained by projecting out the other three closed channels [10, 11]:

$$K_{eff}^c = K_{oo}^c + K_{oc}^c (\chi^c - K_{cc}^c)^{-1} K_{co}^c. \quad (3)$$

where $\chi^c(E)$ is defined through the large-R asymptotic behaviors of the negative energy solutions of f^c and g^c for the C_6 long-range interactions [10], which are -0.8155366, 2.5661999, and 2.5668389 for the $\{F = 2, m_F = -2; F = 2, m_F = -2\}$, $\{F = 2, m_F = -2; F = 3, m_F = -2\}$ and $\{F = 2, m_F = -1; F = 3, m_F = -3\}$ closed channels,

respectively. Using the analytical solutions of C_6 interaction potential, the scattering length can be expressed as [10]:

$$a_{\{q1; q2\}} = \frac{2^{2/3} \pi}{[\Gamma(1/4)]^2} \frac{K_{eff}^c + \tan(\pi/8)}{K_{eff}^c - \tan(\pi/8)} (2\mu C_6 / \hbar^2)^{1/4}. \quad (4)$$

Then if the $\{\mu_s, \mu_t\}$ and the C_6 are given, the scattering length can be obtained by applying the above calculation. The resulting scattering lengths are summarized in the Table I and II by adopting different set of $\{\mu_s, \mu_t\}$ with various conditions.

* hexd@wipm.ac.cn

† xiang.gao@tuwien.ac.at

‡ mszhan@wipm.ac.cn

- [1] U. Fano, Quantum defect theory of l uncoupling in H_2 as an example of channel-interaction treatment, Phys. Rev. A **2**, 353 (1970).
- [2] C. M. Lee, and K. T. Lu, Spectroscopy and Collision Theory. II. The Ar Absorption Spectrum, Phys. Rev. A **8**, 1241 (1973).
- [3] B. Gao, Theory of slow-atom collisions, Phys. Rev. A **54**, 2022 (1996).
- [4] C. M. Lee, Multichannel photodetachment theory, Phys. Rev. A **11**, 1692 (1975).
- [5] Ch. Jungen, and G. Raseev, Spin-electronic-rotational frame transformation for photoionization and Rydberg spectra of diatomic molecules, Phys. Rev. A **57**, 2407 (1998).
- [6] X. Gao, W. H. Zhang, Y. X. Mo, and J. M. Li, Application of multichannel quantum defect theory to unveil quantum interferences in dissociation of superexcited F_2 , Phys. Rev. A **82**, 031401(R) (2010).
- [7] S. Dong, Y. Cui, C. Shen, Y. Wu, M. K. Tey, L. You, and B. Gao, Observation of broad p -wave Feshbach resonances in ultracold ^{85}Rb - ^{87}Rb mixtures, Phys. Rev. A **94**, 062702 (2016).
- [8] Y. Cui, C. Shen, M. Deng, S. Dong, C. Chen, R. L. B. Gao, M. K. Tey, and L. You, Observation of Broad d -Wave Feshbach Resonances with a Triplet Structure, Phys. Rev. Lett. **119**, 203402 (2017).
- [9] C. H. Greene, and Ch. Jungen, Molecular Applications of Quantum Defect Theory, Adv. At. Mol. Phys. **21**, 51 (1985).
- [10] B. Gao, E. Tiesinga, C. J. Williams, and P. S. Julienne, Multichannel quantum-defect theory for slow atomic collisions, Phys. Rev. A **72**, 042719 (2005).
- [11] J. P. Burke, C. H. Greene, and J. L. Bohn, Multichannel Cold Collisions: Simple Dependences on Energy and Magnetic Field, Phys. Rev. Lett. **81**, 3355 (1998).